Journal of Inflammation Research

Dovepress
Taylor & Francis Group

Open Access Full Text Article

ORIGINAL RESEARCH

The EZH2 Inhibitor GSK126 Alleviates Thromboinflammation in Deep Vein Thrombosis by Suppressing TLR4 Signaling via H3K27me3 Modulation

Rudan Zhou[1], Ji Luo[2], Hongyu Zheng[3]

[1]Xenotransplantation Research Institute, the First Affiliated Hospital of Kunming Medical University, Kunming, Yunnan, 650032, People's Republic of China; [2]Department of Intensive Care Unit, West China ZiYang Central Hospital, Ziyang, Sichuan, 641300, People's Republic of China; [3]Department of Trauma Center, the First Affiliated Hospital of Kunming Medical University, Kunming, Yunnan, 650032, People's Republic of China

Correspondence: Hongyu Zheng, Department of Trauma Center, the First Affiliated Hospital of Kunming Medical University, 295 Xichang Road, Wuhua, Kunming, Yunnan, 650032, People's Republic of China, Tel +86 138 8850 2190, Email zhenghongyu@kmmu.edu.cn

Background: Deep vein thrombosis (DVT) is characterized by abnormal clot formation, often accompanied by endothelial dysfunction and inflammation. Among various inflammatory mediators, extracellular histone H3—acting as a damage-associated molecular pattern (DAMP)—has been implicated in DVT pathogenesis by activating Toll-like receptor 4 (TLR4). Enhancer of zeste homolog 2 (EZH2), a histone methyltransferase, regulates gene expression via H3K27me3. Because TLR4 transcription may be epigenetically modulated, this study aimed to evaluate whether GSK126, an EZH2 inhibitor, mitigates DVT by modulating H3K27me3 and suppressing TLR4 signaling.

Methods: To evaluate whether GSK126 attenuates histone H3-exacerbated thromboinflammation in vivo, we employed a stenosis-induced DVT mouse model combined with exogenous histone H3 injection. *Tlr4*-deficient (*Tlr4*$^{-/-}$) mice were used to assess the role of TLR4 signaling in thrombus formation and inflammation. GSK126 was administered intraperitoneally, and thrombus burden along with inflammatory gene expression were quantified. In vitro, human umbilical vein endothelial cells (HUVECs) were stimulated with lipopolysaccharide (LPS) and treated with GSK126, either alone or in combination with the TLR4-specific inhibitor TAK-242. *TLR4* mRNA and protein levels, as well as downstream inflammatory signaling, were analyzed using qPCR and Western blotting.

Results: GSK126 significantly reduced thrombus burden, TLR4 expression, and inflammatory mediators in vivo. In endothelial cells, GSK126 decreased TLR4 and phosphorylated IκBα levels, which was consistently accompanied by reduced H3K27me3 levels. Co-treatment with TAK-242 enhanced these effects. These findings suggest that GSK126 alleviates TLR4-mediated inflammation, likely through its modulation of histone methylation, specifically H3K27me3.

Conclusion: Our results support a role for TLR4 signaling in DVT pathogenesis and suggest that EZH2 inhibition with GSK126 may represent a novel therapeutic approach to thromboinflammation by modulating H3K27me3 and suppressing TLR4-driven inflammatory pathways.

Plain Language Summary: Deep vein thrombosis (DVT) is a serious condition where abnormal blood clots form in veins, often leading to swelling, pain, and sometimes life-threatening complications. Inflammation and immune responses play a major role in the formation of these clots. One key protein involved in this process is TLR4, which is activated by certain molecules released from damaged cells.

In this study, researchers explored whether blocking a specific enzyme called EZH2 could help reduce clot-related inflammation. EZH2 can modify DNA packaging in cells through a marker known as H3K27me3, potentially influencing the activity of TLR4.

The team tested an EZH2 inhibitor called GSK126 in a mouse model of DVT. They found that treatment with GSK126 led to smaller clots and lower levels of TLR4 and other inflammation-related molecules. Similar results were seen in human endothelial cells grown in the lab. When combined with a TLR4-specific blocker, the anti-inflammatory effects were even stronger.

Received: 3 July 2025
Accepted: 19 September 2025
Published: 2 October 2025

These results suggest that targeting EZH2 using GSK126 may help reduce harmful inflammation in DVT by lowering TLR4 activity. This approach could offer a new potential therapy for patients with clot-related inflammatory diseases in the future.

Keywords: deep vein thrombosis, EZH2, GSK126, TLR4 signaling, H3K27me3, thromboinflammation

Introduction

Deep vein thrombosis (DVT) is a condition characterized by abnormal clotting of blood within deep veins, typically in the lower extremities. DVT is a critical public health concern worldwide, largely due to its severe complications, including pulmonary embolism (PE). In the United States alone, PE accounts for more than 300,000 deaths annually, highlighting the global burden of this condition.[1]

The pathogenesis of DVT is classically explained by Virchow's triad: hemostasis, hypercoagulability, and vascular endothelial damage.[2,3] Although advances have been made in understanding its mechanisms, both diagnosis and treatment of this condition have major challenges. Although tools such as D-dimer testing and imaging (CT, ultrasound) are commonly used,[4,5] they still have limitations in sensitivity, specificity, accessibility, or associated risks, particularly in detecting distal or asymptomatic thrombi.

In contrast, ultrasound is noninvasive and widely available, but its limited sensitivity for detecting distal or deep-seated thrombi and operator dependency often lead to variable diagnostic outcomes.[5]

Current therapies, including anticoagulants and inferior vena cava (IVC) filters, reduce thrombus burden and prevent embolism but are limited by bleeding risks and procedural complications.[6–8] These limitations underscore the need to better understand DVT pathogenesis at the molecular level and to identify novel therapeutic targets.

Recent studies have revealed that inflammatory responses play a critical role in DVT pathogenesis. Among these, extracellular histones, particularly H3 and H4, act as damage-associated molecular patterns (DAMPs) that activate TLR4 and TLR2, inducing proinflammatory cytokine release and exacerbating vascular endothelial damage.[8] Notably, citrullinated histone H3 (CitH3), a hallmark of neutrophil extracellular traps (NETs), is closely associated with prothrombotic processes linked to NET formation.[9,10] Elevated CitH3 levels have been found in DVT patients, suggesting its potential as a diagnostic biomarker.[11] CitH3, a component of neutrophil extracellular traps, has been implicated in promoting inflammation in DVT. One potential mechanism mediating this effect is through the activation of Toll-like receptor 4 (TLR4) signaling, which drives downstream inflammatory responses.

TLR4 links inflammation to thrombosis by activating intracellular pathways such as the activating nuclear factor kappa B (NF-κB) and mitogen-activated protein kinase (MAPK) pathways, which promote the expression of proinflammatory cytokines and adhesion molecules.[12,13] Additionally, TLR4 activation contributes to venous thrombus resolution by promoting leukocyte infiltration and MMP-9 activity,[14] whereas excessive TLR4 activation exacerbates endothelial damage through oxidative stress.[15] Collectively, these prior studies highlight TLR4 as a critical regulator of thromboinflammatory responses in DVT.

Epigenetic regulation, particularly via enhancer of zeste homolog 2 (EZH2), has been implicated in controlling inflammatory signaling pathways.[16,17] As a histone methyltransferase responsible for H3K27me3, EZH2 has been reported to suppress the expression of Toll-interacting protein (Tollip), a negative regulator of TLR4 signaling.[17] By silencing this inhibitory feedback mechanism, EZH2 may enhance TLR4-mediated inflammatory responses. Therefore, pharmacological inhibition of EZH2 could attenuate thromboinflammation by restoring negative regulation within the TLR4 signaling pathway. GSK126, a selective EZH2 inhibitor, has shown promise in reducing inflammation and thrombosis by modulating inflammatory signaling pathways.[18] Although this molecule has been studied primarily in cancer and other inflammatory conditions, its effects on TLR4 activity suggest broader applications, including in those related to DVT.

Given the regulatory role of EZH2 in TLR4-related inflammatory signaling, we hypothesized that pharmacological inhibition of EZH2 could attenuate thromboinflammation in DVT. Therefore, in this study, we investigated whether GSK126, a selective EZH2 inhibitor, modulates histone methylation (H3K27me3) and suppresses TLR4-mediated

inflammatory responses in a DVT model. Our findings provide new insights into the epigenetic regulation of vascular inflammation and identify EZH2 inhibition as a potential therapeutic strategy in DVT.

Methods

Construction of the DVT Mouse Model

Ten-week-old male C57BL/6J mice (18–22 g) and *Tlr4*$^{-/-}$ mice were used in this study. C57BL/6J mice were purchased from the Experimental Animal Center of Kunming Medical University, and *Tlr4*$^{-/-}$ mice were obtained from Cyagen (Suzhou) Biotechnology Co., Ltd. [License number: SYXK(Dian) K2020-0006]. All protocols were approved by the Institutional Animal Care and Use Committee (IACUC) of Kunming Medical University (Approval No. KMMU20221518).

To induce DVT, mice were anesthetized with 2% isoflurane and placed in the supine position. Following a midline laparotomy, the inferior vena cava (IVC) was exposed. All visible side branches between the renal and iliac veins were ligated with 7–0 silk sutures. A partial ligation was then performed just below the renal veins using a 5–0 silk suture tied around the IVC over a 30-gauge needle, which was then removed to create IVC stenosis. The abdominal wall was closed in layers, and mice were monitored postoperatively on a warming pad.

The study included six experimental groups involving both wild-type and *Tlr4*$^{-/-}$ mice. Treatments included GSK126 (50 mg/kg, i.p., daily for 7 days prior to surgery) and/or histone H3 (20 μg/mouse, i.p., 24 hours prior to surgery). DVT was induced on Day 0, and all animals were euthanized 24 hours post-surgery for blood and tissue collection. Thrombus and IVC wall were carefully isolated, excluding surrounding connective, lymphatic, or arterial tissue.

Each group was initially planned to include 10 animals based on prior literature and feasibility testing. However, due to surgical variability and occasional model failure, the final number of animals analyzed per group ranged from 6 to 10.

A schematic timeline of the experimental design is provided in Supplementary Figure S1, and a detailed summary of treatment regimens and group allocation is shown in Supplementary Table S1.

Successful model induction was confirmed at 24 h post-surgery by the presence of visible thrombi in the IVC, often accompanied by vessel swelling and a purplish discoloration of the venous wall. Thrombus weight and length were recorded in all animals. Furthermore, representative molecular and histological markers of thrombosis and inflammation—including elevated levels of *Il6, Vcam1*, *Vwf*, and *Sele* were assessed to validate the biological relevance of the model.

Immunofluorescence (IF)

After dewaxing and hydration, antigen retrieval was performed using citrate-based retrieval solution (Beyotime, P0090) in a microwave oven for 25 minutes, followed by natural cooling. The sections were blocked with 5% normal goat serum (prepared with 0.3% Triton X-100 and diluted to 5% with PBS) for 1 hour at room temperature. Subsequently, sections were incubated overnight at 4°C with the primary antibodies anti-CD31 (mouse, Invitrogen, MA1-80069, 1:100) and anti-VCAM-1 (rabbit, Invitrogen, PA5-86042, 1:150), diluted in 2% goat serum solution. After five washes with PBST (0.01 M PBS with 0.1% Tween 20), the sections were incubated for 1 hour at 37°C in the dark with the fluorescently conjugated secondary antibodies Cy3-labeled goat anti-rabbit IgG (KPL, 072–01-15-06, 1:1000) and DyLight 488-labeled goat anti-mouse IgG (KPL, 5230–0391, 1:1000). Nuclei were counterstained with DAPI (Beyotime, C1005) for 5 minutes. The sections were mounted with antifade mounting medium (Beyotime, P0126) and observed under a fluorescence microscope. Images were acquired and analyzed using ImageJ software.

Real-Time Quantitative Polymerase Chain Reaction (qRT–PCR)

Total RNA was extracted from 40 mg of tissue using 500 μL of TRIzol lysis buffer (Invitrogen, 15596026), and the mixture was subsequently lysed on ice for 15 minutes. After addition of 100 μL of chloroform (Sinopharm, 10009618), the mixture was centrifuged at 4°C for 15 minutes at 12,000 rpm, and the supernatant was collected. The RNA was precipitated by adding an equal volume of isopropanol (Sinopharm, 10009268), washed with 75% ethanol, and dissolved in DEPC water. The RNA sample was mixed with 2 μL of 5×gDNA Buffer and RNase-free ddH_2O to a final volume of 10 μL, vortexed gently, and incubated at 42°C for 3 minutes to remove gDNA.

Table 1 Primer Sequence

Gene	Primer Name	Sequence (5'→3')	Product Length (bp)
β-actin	β-actin-F	CTGGAGAAGAGCTATGAG	141
β-actin	β-actin-R	GATGGAATTGAATGTAGTTTC	
Tlr4	Tlr4-F	CAATCGCATAGAGACATC	155
Tlr4	Tlr4-R	GTTCAACATTCACCAAGA	
Sele	Sele-F	AATGACGAGAGATGTAAC	111
Sele	Sele-R	GGTGTAACTATTGATGGT	
Vcam1	Vcam1-F	AATACTACACTCACCTTCAT	83
Vcam1	Vcam1-R	CTAATTCCAGCCTCGTTA	
Vwf	Vwf-F	TGGCTCCTCTATGTTGTC	77
Vwf	Vwf-R	TGTGTAACCTCTCCATCAT	
Il6	Il6-F	ACCTGTCTATACCACTTC	117
Il6	Il6-R	GCATCATCGTTGTTCATA	

Subsequently, 2 μL of 10×King RT Buffer, 1 μL of FastKing RT Enzyme Mix, 2 μL of FQ-RT Primer Mix, and 5 μL of RNase-free ddH2O were added to bring the final volume to 20 μL. The mixture was incubated at 42°C for 15 minutes, followed by 95°C for 3 minutes to terminate the reaction. qPCR was performed on an ABI 7500 system (Thermo Fisher) with 5 μL of Taq Pro Universal SYBR qPCR Master Mix (Vazyme, Q712-02), 0.25 μL of primers, and 1 μL of cDNA template, with a total volume of 10 μL. The PCR program consisted of predenaturation at 95°C for 10 minutes, followed by 40–45 cycles of 95°C for 15 seconds and 60°C for 30 seconds. Relative expression was calculated using the 2-ΔΔCt method, with *β-actin* used as the internal reference. The primer sequences are shown in Table 1.

Flow Cytometry Analysis

To investigate the role of Tlr4 in extracellular histone H3-induced platelet activation, peripheral blood was collected from mice in the DVT model groups (DVT, DVT + H3, $Tlr4^{-/-}$,and $Tlr4^{-/-}$DVT + H3 groups) in the third experiment for flow cytometry analysis of platelet activation. For this analysis, the experimental groups were designated as follows: (1) DVT–PRP group (wild-type mice with platelet-rich plasma treatment), (2) DVT + H3–PRP group (wild-type mice treated with a calf thymus-derived histone mixture containing histone H3; Macklin, H920439, 20 μg/mouse), (3) *Tlr4*−/¯–PRP group (*Tlr4* knockout mice with PRP treatment), and (4) $Tlr4^{-/-}$ DVT + H3 group (*Tlr4* knockout mice treated with the same histone mixture).

Peripheral blood was collected from the mice into tubes containing sodium citrate as an anticoagulant. The blood samples were centrifuged at 180 × g for 10 minutes to collect the supernatant, followed by centrifugation at 3000 × g for 15 minutes to obtain platelet-rich plasma (PRP). The platelets were resuspended in 2 mL of PBS and recentrifuged at 3000 × g for 15 minutes. The final pellet was resuspended in 200 μL of PBS and divided into two portions: one was incubated with 1 μg of FITC-conjugated anti-CD61 antibody (Thermo Fisher, 11–0611-82; 1:100 dilution), and the other with 0.25 μg of PE-conjugated anti-CD62P antibody (Thermo Fisher, 12–0626-82; 1:200 dilution). Flow cytometry data were acquired using a NovoCyte Advanteon flow cytometer (Agilent, USA). Representative gating plots are shown in Supplementary Figure S2.

Cell Culture

Human umbilical vein endothelial cells (HUVECs, BNCC342438) were purchased from BeNa Culture Collection. The cells were divided into four groups: (1) HUVEC control group; (2) HUVECs treated with 1 μg/mL lipopolysaccharide

(LPS, Sigma-Aldrich, L2880); (3) HUVECs treated with 1 μg/mL LPS and 10 μM GSK126; and (4) HUVECs treated with 1 μg/mL LPS, 10 μM GSK126, and 50 nM TAK-242 (MCE, HY-11109). LPS (1 μg/mL) was used to simulate endothelial inflammatory activation.

Each group of cells was first treated with GSK126 (10 μM) or TAK-242 (50 nM) for 24 hours and then stimulated with 1 μg/mL LPS for 6 hours. The cell pellets and culture supernatants were collected for subsequent detection. Additional in vitro assays using the same treatment groups, included quantitative PCR to assess *TLR4* mRNA expression and Western blotting to determine protein levels of TLR4, phosphorylated IκBα, and H3K27me3.

CCK-8 Detection

After culture, three replicate wells were set for each group of cells, and cell activity was determined via a CCK-8 kit (Dojindo, CK04). Ten microliters of CCK-8 solution was added to each well and incubated at 37°C for 2 hours, and the OD value was measured at 450 nm to evaluate the effects of different treatments on cell activity.

Enzyme-Linked Immunosorbent Assay (ELISA) Analysis

The cell culture supernatant from each group was collected, with 3 replicates. The levels of the inflammatory factors IL-6 and TNF-α were determined using ELISA kits (Elabscience, E-EL-H6156, and E-EL-H0109). The OD value was measured at 450 nm, and the concentrations of IL-6 and TNF-α were determined via a standard curve.

Western Blot Detection

Cells were collected and lysed in RIPA lysis buffer (Beyotime, P0013B), and total protein was extracted from three biological replicates. Equal amounts of protein were separated by SDS–PAGE and transferred to PVDF membranes. The membranes were blocked and then incubated overnight at 4°C with primary antibodies against TLR4 (Cell Signaling Technology, 14358, 1:1000), P-selectin (Bioss, bs-0561R, 1:1000), ICAM-1 (Bioss, bs-0608R, 1:2000), phosphorylated IκBα (Proteintech, 82349-1-RR, 1:4000), H3K27me3 (Proteintech, 61018, 1:500), and β-Actin (ZSGB-Bio, TA-09, 1:2000). After washing, the membranes were incubated with HRP-conjugated secondary antibodies, including anti-mouse IgG-HRP (Abmart, M21001L, 1:4000) and anti-rabbit IgG-HRP (Abmart, M21002L, 1:4000), according to the host species of the primary antibodies. Protein bands were visualized using an enhanced chemiluminescence (ECL) detection system (NCM Biotech, P10100), and band intensities were quantified using ImageJ software.

Statistical Analysis

All data were repeated at least three times and analyzed using GraphPad Prism 9.0 (GraphPad Software, CA, USA). Normal distribution was verified using the Shapiro–Wilk test, and homogeneity of variance was assessed by the Levene test. Comparisons between two groups were performed using a two-tailed Student's t tests; multiple group comparisons were performed by one-way ANOVA followed by Tukey's post hoc test. The F value and P value for ANOVA are reported. The data are presented as the means ± standard deviations (SDs), and statistical significance was set at $p < 0.05$. Significant marks: *$p < 0.05$, **$p < 0.01$, ***$p < 0.001$.

All in vitro experiments were independently repeated at least three times using separate cell passages.

Results

GSK126 Alleviates DVT Formation by Downregulating *Tlr4* Expression

GSK126 treatment significantly downregulated *Tlr4* expression and reduced thrombus weight in a mouse DVT model ($p < 0.01$). These findings suggest that suppression of *Tlr4* contributes to the therapeutic effects of GSK126.

To confirm successful induction of the DVT model and evaluate the effect of GSK126 on thrombus formation, we first measured thrombus weights in different experimental groups (Figure 1A). Thrombus weight was significantly increased in the DVT group compared with the blank group, and GSK126 treatment markedly reduced thrombus formation ($p < 0.0001$); however, thrombus weight in the DVT+GSK126 group remained higher than that in the blank group.

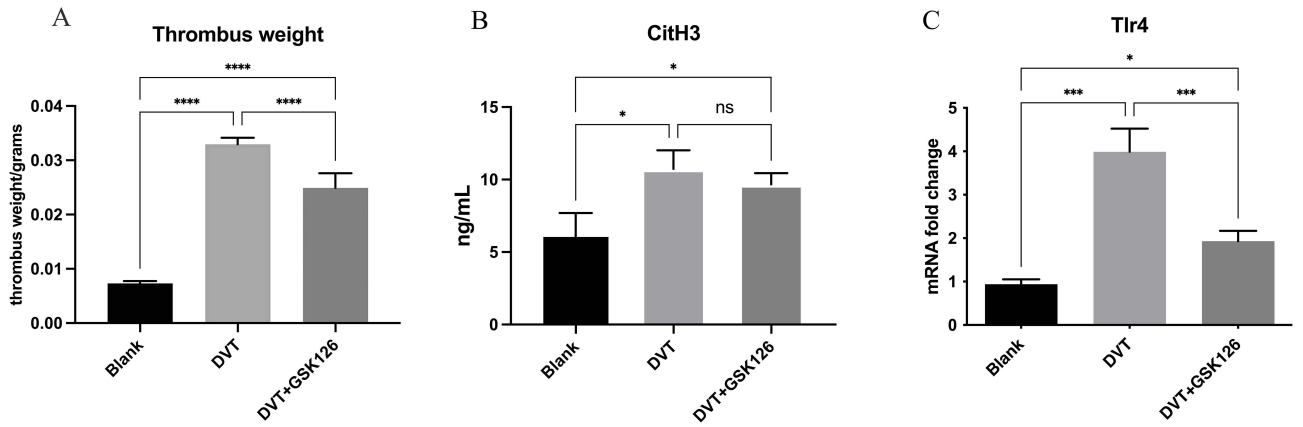

Figure 1 GSK126 reduces thrombus formation and modulates inflammatory responses in a murine DVT model.(**A**) Thrombus weight in the blank, DVT, and DVT+GSK126 groups. Thrombus weight was significantly increased in the DVT group compared with the blank group (****$p < 0.0001$), and significantly reduced in the DVT+GSK126 group (****$p < 0.0001$ vs DVT). However, thrombus weight in the DVT+GSK126 group remained significantly higher than in the blank group (****$p < 0.0001$).(**B**) Plasma CitH3 levels in the three groups. CitH3 was significantly elevated in the DVT group compared with the blank group (*$p < 0.05$). GSK126 treatment did not significantly reduce CitH3 levels compared with the DVT group (ns), but CitH3 levels in the DVT+GSK126 group remained significantly higher than in the blank group (*$p < 0.05$).(**C**) *Tlr4* mRNA expression. *Tlr4* expression was significantly increased in the DVT group compared with the blank group (***$p < 0.001$), and significantly reduced by GSK126 treatment (*$p < 0.05$ vs DVT). However, levels in the DVT+GSK126 group remained significantly higher than in the blank group (***$p < 0.001$).
Note: *p < 0.05, ***p < 0.001, ****p < 0.0001; ns, not significant.

We next assessed plasma CitH3 concentrations (Figure 1B). Consistent with previous reports in DVT patients, CitH3 levels were significantly elevated in the DVT group ($p < 0.05$). However, GSK126 treatment did not significantly alter plasma CitH3 concentrations ($p > 0.05$).

Finally, we examined *Tlr4* mRNA expression levels (Figure 1C). In the DVT group, *Tlr4* expression was significantly upregulated ($p < 0.001$), suggesting increased activity of the *Tlr4* signaling pathway during thrombus formation. GSK126 treatment significantly reduced *Tlr4* expression ($p < 0.05$), although levels remained higher than those of the blank group. These findings indicate that GSK126 partially suppresses *Tlr4* expression in the DVT model.

GSK126 Treatment and *Tlr4* Deficiency Mitigate H3-Induced Thromboinflammation in DVT

Both GSK126 treatment and *Tlr4* deficiency significantly reduced H3-induced thrombus formation and vascular inflammation, implicating *Tlr4* as a key mediator of H3-driven thromboinflammatory responses. To evaluate the roles of *Tlr4* signaling and GSK126 in regulating inflammatory responses and thrombosis in DVT models, we analyzed the thrombus weight, plasma markers, endothelial integrity, and inflammatory gene expression across the experimental groups.

The thrombus weight was significantly greater in the DVT+H3 group than in the DVT group ($p < 0.0001$), demonstrating that exogenous H3 exacerbates thrombosis (Figure 2A). In the $Tlr4^{-/-}$ mice, the thrombus weight in the DVT+H3 group was significantly lower than that in the WT DVT+H3 group ($p < 0.0001$), indicating that the prothrombotic effect of H3 is dependent on *Tlr4* signaling. The thrombus weight in the $Tlr4^{-/-}$ + H3 group was comparable to that in the DVT group (ns), confirming that, in the absence of *Tlr4*, H3 fails to promote thrombosis. These comparisons collectively suggest that the prothrombotic effect of H3 is primarily mediated by *Tlr4* signaling. Compared with the control treatment, the GSK126 treatment significantly reduced the thrombus weight in both the DVT +GSK126 and DVT+H3+GSK126 groups (****$p < 0.0001$), highlighting its ability to mitigate thrombosis. These findings indicate that H3 promotes thrombosis through *Tlr4*-mediated signaling and that GSK126 effectively alleviates thrombosis by targeting this pathway.

The thrombus weight–to-length ratio showed distinct trends across groups (Figure 2B). Exogenous H3 did not significantly alter the thrombus weight-to-length ratio compared with that in the DVT group (DVT vs DVT+H3, ns), indicating that its prothrombotic effects primarily increase the thrombus weight without affecting the thrombus density. In contrast, GSK126 treatment significantly reduced the thrombus weight–length ratio in both the DVT+GSK126 and

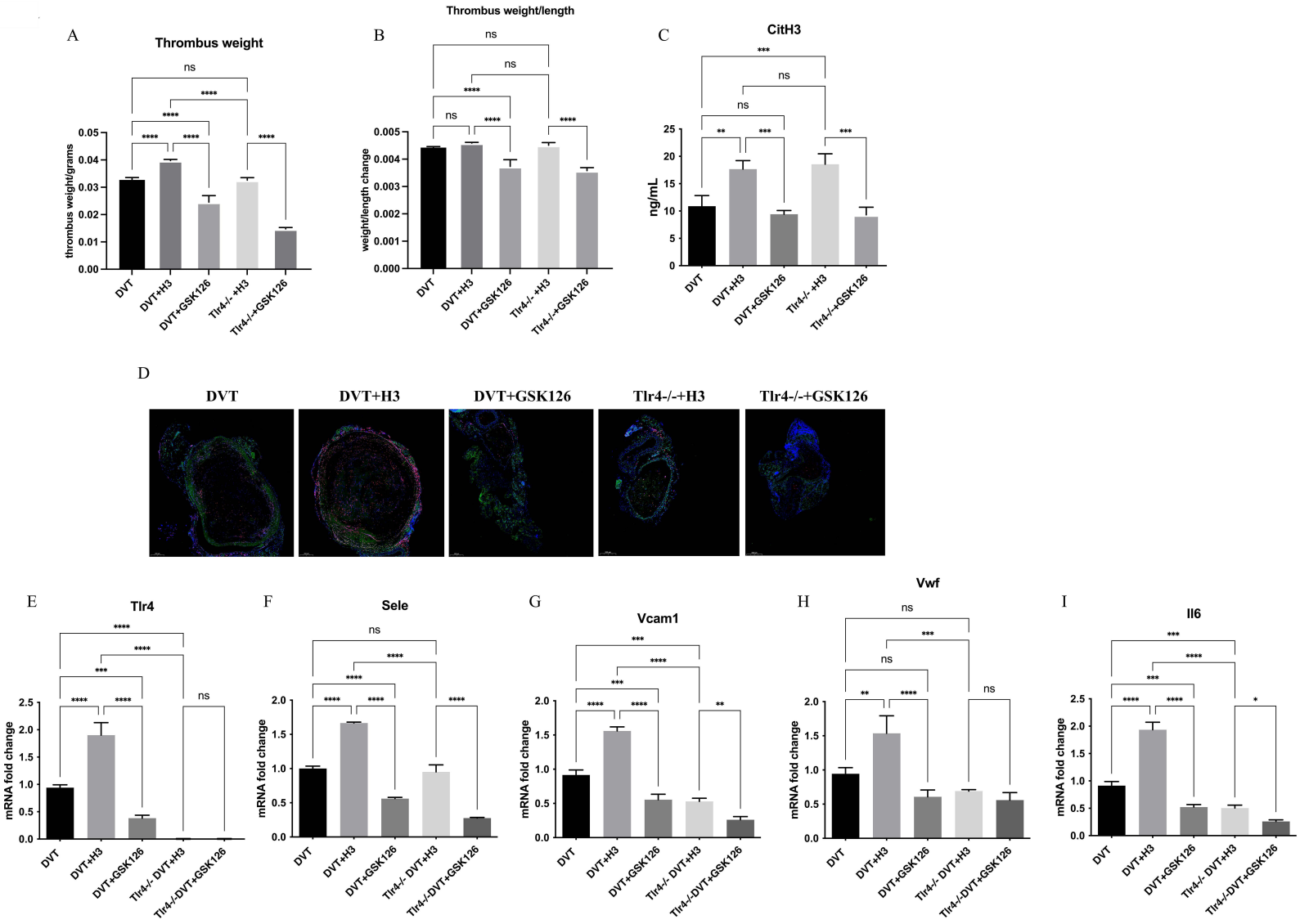

Figure 2 GSK126 treatment and *Tlr4* deficiency mitigate thrombus formation and endothelial injury in a murine DVT model. (**A**) Thrombus weight. Thrombus weight was significantly increased in the DVT+H3 group compared with the DVT group (****$p < 0.0001$). This increase was significantly mitigated by GSK126 treatment and in *Tlr4*-deficient mice (****$p < 0.0001$ vs DVT+H3). (**B**) Thrombus weight-to-length ratio. Exogenous H3 did not significantly alter the ratio compared with the DVT group (ns vs DVT). In contrast, GSK126 treatment significantly reduced the ratio compared with the DVT+H3 group (****$p < 0.0001$). Similarly, Tlr4-/-+GSK126 treatment significantly reduced the ratio compared to the $Tlr4^{-/-}$+H3 group (****$p < 0.0001$). (**C**) Plasma CitH3 levels. CitH3 levels were significantly elevated in the DVT+H3 group compared with the DVT group ($p < 0.01$). This elevation was significantly reduced by GSK126 treatment (***$p < 0.001$ vs DVT+H3) but was not significantly altered in $Tlr4^{-/-}$ mice (ns vs DVT+H3). (**D**) Immunofluorescence staining of vein sections for CD31 (green) and VCAM1 (red), showing endothelial injury and adhesion molecule expression. (**E**) *Tlr4* mRNA expression. *Tlr4* mRNA levels were significantly increased in the DVT+H3 group compared with the DVT group (****$p < 0.0001$). This increase was significantly reduced by GSK126 treatment or in *Tlr4*-deficient mice (****$p < 0.0001$ vs DVT+H3).(**F–I**) Expression of inflammatory genes including *Sele* (**F**), *Vcam1* (**G**), *Vwf* (**H**), and *Il6* (**I**). All genes were significantly upregulated in the DVT+H3 group compared with the DVT group (****$p < 0.0001$ for *Sele*, *Vcam1*, and *Il6*; **$p < 0.01$ for *Vwf*). The expression levels of *Sele* and *Vwf* were significantly higher in the DVT+H3 group than in the $Tlr4^{-/-}$ + H3 and DVT groups. GSK126 treatment significantly reduced the expression of these genes, with significant reductions observed for each gene. The upregulation of *Il6* and *Vcam1* was attenuated in $Tlr4^{-/-}$ mice (****$p < 0.0001$ vs DVT+H3).

Note: *p<0.05; **p<0.01; ***p<0.001; ****p<0.0001; ns, not significant Statistical analysis was performed for pairwise comparisons between groups with the same baseline genotype and treatment conditions.

https://doi.org/10.2147/JIR.S551388

Tlr4$^{-/-}$+GSK126 groups ($p < 0.0001$), further supporting its role in reducing the thrombus burden, likely through anti-inflammatory and antithrombotic mechanisms.

Compared with those in the DVT group, plasma CitH3 levels were significantly elevated in the DVT+H3 group ($p < 0.01$), demonstrating that exogenous H3 administration increases circulating histone H3 levels (Figure 2C). Compared with those in the DVT group, the plasma CitH3 levels in the *Tlr4*$^{-/-}$ DVT+H3 group were similarly elevated ($p < 0.001$).

To assess endothelial integrity and inflammation, we performed immunofluorescence staining for CD31 and VCAM1 (Figure 2D). VCAM1 expression was significantly upregulated in the DVT group, indicating vascular inflammation, whereas CD31 staining was disrupted, reflecting endothelial damage. In the GSK126-treated and *Tlr4*$^{-/-}$ groups, Vcam1 expression was markedly reduced, with the CD31 distribution appearing more continuous, suggesting that both interventions preserve endothelial integrity and mitigate vascular inflammation.

Compared with that in the DVT group, the expression of proinflammatory and thrombogenic genes, including *Tlr4*, *Sele*, *Vcam1*, *Vwf* and *Il6* was significantly greater in the DVT+H3 group (Figure 2E–I). The expression levels of *Sele* and *Vwf* were significantly higher in the DVT+H3 group than in the *Tlr4*$^{-/-}$ +H3 and DVT groups, whereas no significant difference was observed between the latter two groups. Inflammatory markers such as *Il-6* and *Vcam1* were significantly upregulated by H3 stimulation, and this upregulation was attenuated in *Tlr4*$^{-/-}$ mice. GSK126 treatment significantly reduced the expression of these genes in both the WT and *Tlr4*$^{-/-}$ groups ($p < 0.01$). These findings suggest that GSK126 mitigates thromboinflammatory responses primarily by downregulating *Tlr4* and its downstream targets.

Tlr4 Mediates H3-Induced Upregulation of Adhesion Molecules in a DVT Model

Histone H3 upregulated platelet and endothelial adhesion molecules in a *Tlr4*-dependent manner, as shown by the significant reduction of this effect in *Tlr*4-deficient mice. To investigate the role of *Tlr4* in the extracellular histone H3-induced upregulation of adhesion molecules, we analyzed the expression of P-selectin and integrin αIIbβ3 across the experimental groups (Figure 3).

The expression of P-selectin (Figure 3A), a key adhesion molecule involved in platelet activation and inflammatory responses, was significantly greater in the WT-PRP+H3 group than in the WT-PRP group ($p < 0.0001$). Conversely, P-selectin expression was significantly reduced in the *Tlr4*$^{-/-}$ PRP+H3 group ($p < 0.001$), and further reduced in the *Tlr4*$^{-/-}$ + GSK126 group ($p < 0.0001$), indicating that *Tlr4* is **a** major contributor to the H3-induced upregulation of P-selectin.

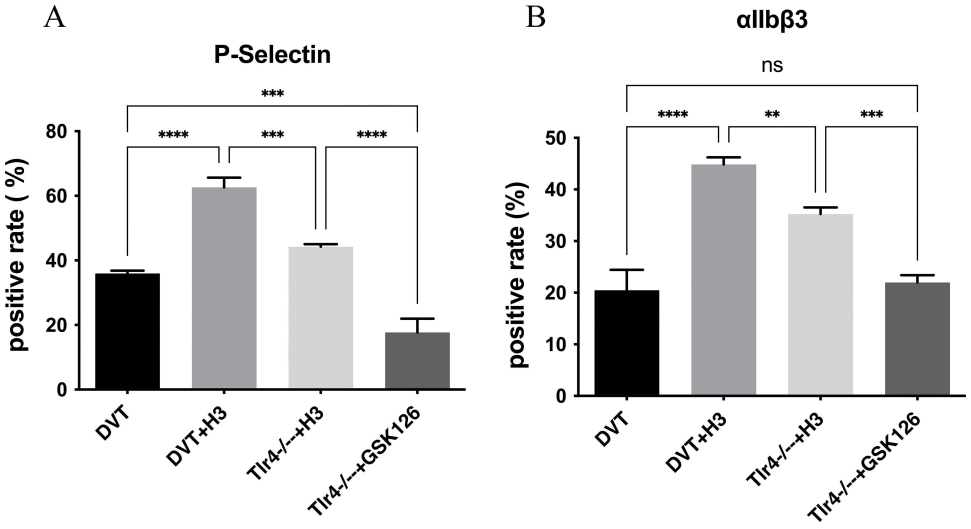

Figure 3 *Tlr4* mediates H3-induced upregulation of platelet adhesion markers. (**A** and **B**) Expression levels of platelet adhesion markers P-selectin (**A**) and integrin αIIbβ3 (**B**). H3 stimulation significantly increased the expression of both P-selectin and integrin αIIbβ3 in platelet-rich plasma (PRP) from WT mice (****$p < 0.0001$ vs WT). The H3-induced upregulation was significantly attenuated in *Tlr4*-deficient mice compared to WT mice (***$p < 0.001$ for P-selectin; **$p < 0.01$ for integrin αIIbβ3; vs WT+H3).
Note: **p < 0.01; ***p < 0.001; ****p < 0.0001; ns, not significant.

Similarly, integrin αIIbβ3 (Figure 3B), which plays a critical role in platelet aggregation and thrombosis, was significantly elevated in the WT-PRP+H3 group compared with the WT-PRP group ($p < 0.0001$), whereas its expression was markedly reduced in the Tlr4-/- PRP+H3 group ($p < 0.01$) and further reduced in the *Tlr4*$^{-/-}$ + GSK126 group ($p < 0.001$). These results further support the role of *Tlr4* in mediating H3-induced upregulation of adhesion molecules.

Taken together, these results underscore the pivotal role of *Tlr4* in the extracellular histone H3-induced upregulation of adhesion molecules, emphasizing its involvement in H3-driven proinflammatory and prothrombotic responses.

GSK126 Suppresses LPS-Induced Inflammation in Endothelial Cells via TLR4 Downregulation

To evaluate whether GSK126 affects cell viability, we performed a CCK-8 assay (Figure 4A). Compared with the control conditions, LPS stimulation slightly increased cell viability, but the difference was not statistically significant ($p > 0.05$). Neither GSK126 treatment nor cotreatment with TAK-242 further affected cell viability ($p > 0.05$), suggesting that the observed effects of GSK126 on inflammatory responses were independent of changes in cell viability.

To assess the effects of GSK126 on inflammatory cytokines, we measured the IL-6 and TNF-α levels in the culture supernatants using ELISAs (Figure 4B and C). LPS stimulation significantly increased the IL-6 and TNF-α levels ($p < 0.0001$), which is consistent with the activation of TLR4-mediated inflammation. Compared with LPS alone, GSK126 treatment significantly reduced IL-6 secretion ($p < 0.01$) and TNF-α levels ($p < 0.001$). Compared with GSK126 alone, the addition of TAK-242 further decreased IL-6 levels ($p < 0.05$); however, levels remained significantly higher than those in the control group ($p < 0.05$). Compared with GSK126 treatment alone, cotreatment with TAK-242 did not result in an additional significant reduction in TNF-α ($p > 0.05$). These findings suggest that GSK126 suppresses the secretion of inflammatory cytokines, particularly IL-6, through TLR4 downregulation, whereas TNF-α regulation may involve pathways other than TLR4.

To further evaluate the effects of GSK126 on the expression of TLR4 and its downstream adhesion molecules, we performed Western blot analysis of TLR4, ICAM-1, and P-selectin (Figure 4D–G). LPS stimulation significantly upregulated the expression of TLR4, ICAM-1, and P-selectin ($p < 0.001$), which is consistent with the TLR4-mediated activation of adhesion molecules. GSK126 treatment significantly reduced TLR4 expression ($p < 0.01$), but TLR4 levels remained higher than those in the control group ($p < 0.05$). Similarly, GSK126 significantly decreased the expression of ICAM-1 and P-selectin ($p < 0.05$), but their levels remained higher than those in the control group ($p < 0.05$). Cotreatment with TAK-242 further suppressed the expression of TLR4, ICAM-1, and P-selectin. While TLR4 levels remained higher than those in the control group ($p < 0.05$), ICAM-1 and P-selectin expression was fully restored to levels comparable to those in the control group ($p > 0.05$).

These results indicate that GSK126 mitigates LPS-induced proinflammatory responses primarily through TLR4 downregulation, which in turn suppresses the upregulation of the downstream adhesion molecules ICAM-1 and P-selectin. Cotreatment with TAK-242 further confirmed the central role of TLR4 in mediating these inflammatory responses.

GSK126 Reduces H3K27me3 and Suppresses TLR4 Signaling in LPS-Stimulated Endothelial Cells

GSK126 reduced global H3K27me3 levels and inhibited TLR4 transcription and downstream NF-κB activation, suggesting a potential epigenetic mechanism of TLR4 regulation. Compared with the control group, LPS stimulation markedly increased *TLR4* mRNA expression ($p < 0.001$), confirming pathway activation (Figure 5A). GSK126 treatment significantly reduced the LPS-induced upregulation ($p < 0.01$), although the level remained higher than that of the control. Importantly, co-treatment with TAK-242 further decreased *TLR4* mRNA expression to a level statistically indistinguishable from that of the control ($p > 0.05$).

Consistent with the qPCR-based transcriptional data shown in Figure 5A, Western blotting revealed that LPS robustly elevated TLR4 and phosphorylated IκBα (p-IκBα) protein levels ($p < 0.0001$, Figure 5B and C). GSK126 significantly

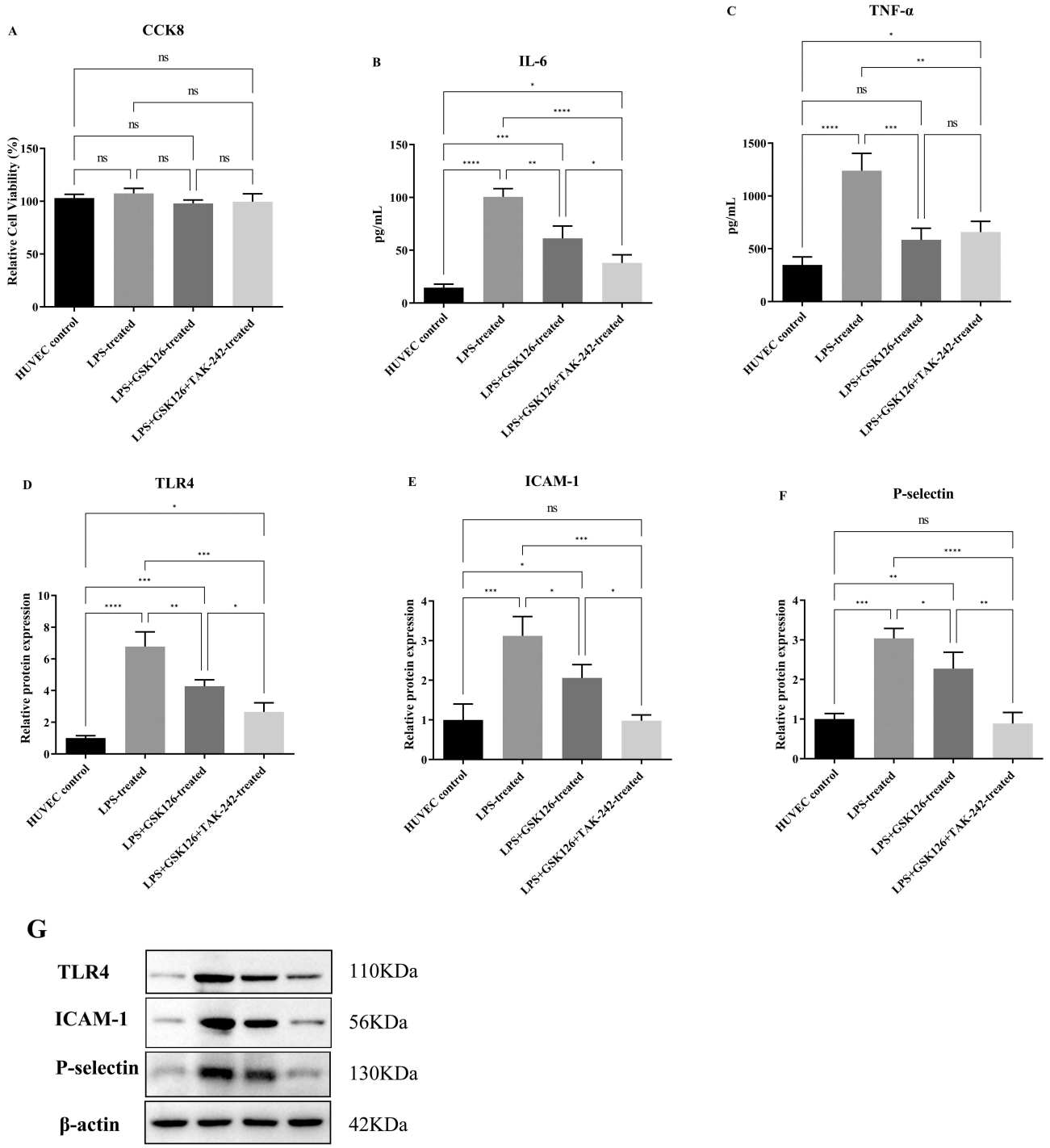

Figure 4 GSK126 suppresses LPS-induced inflammation in endothelial cells via TLR4 downregulation. (**A**) Cell viability assessed by CCK-8 assay. LPS stimulation slightly increased HUVEC viability compared to the control group ($p>0.05$). Neither GSK126 treatment nor cotreatment with TAK-242 significantly altered cell viability ($p>0.05$), suggesting the anti-inflammatory effects were independent of changes in cell viability. (**B** and **C**) ELISA quantification of IL-6 (**B**) and TNF-α (**C**) levels in culture supernatants. LPS stimulation significantly increased the levels of IL-6 and TNF-α (****$p<0.0001$ vs control). Compared with LPS alone, GSK126 treatment significantly reduced IL-6 secretion (**$p<0.01$) and TNF-α levels (***$p<0.001$). Compared with GSK126 alone, the addition of TAK-242 further decreased IL-6 levels (*$p<0.05$); however, cotreatment with TAK-242 did not result in an additional significant reduction in TNF-α ($p>0.05$). (**D**–**F**) Western blot quantification of protein levels. LPS significantly upregulated TLR4 (**D**), ICAM-1 (**E**), and P-selectin (**F**) protein expression (***$p<0.001$ vs control). GSK126 treatment significantly reduced the levels of TLR4 (**$p<0.01$), ICAM-1, and P-selectin (*$p<0.05$ vs LPS). While TLR4 levels remained elevated after cotreatment ($p<0.05$ vs control), ICAM-1 and P-selectin levels were fully restored to baseline (ns vs control). (**G**) Representative immunoblots of TLR4, ICAM-1, and P-selectin, with β-actin as the loading control.

Note: *p<0.05; **p<0.01; ***p<0.001; ****p<0.0001; ns, not significant.

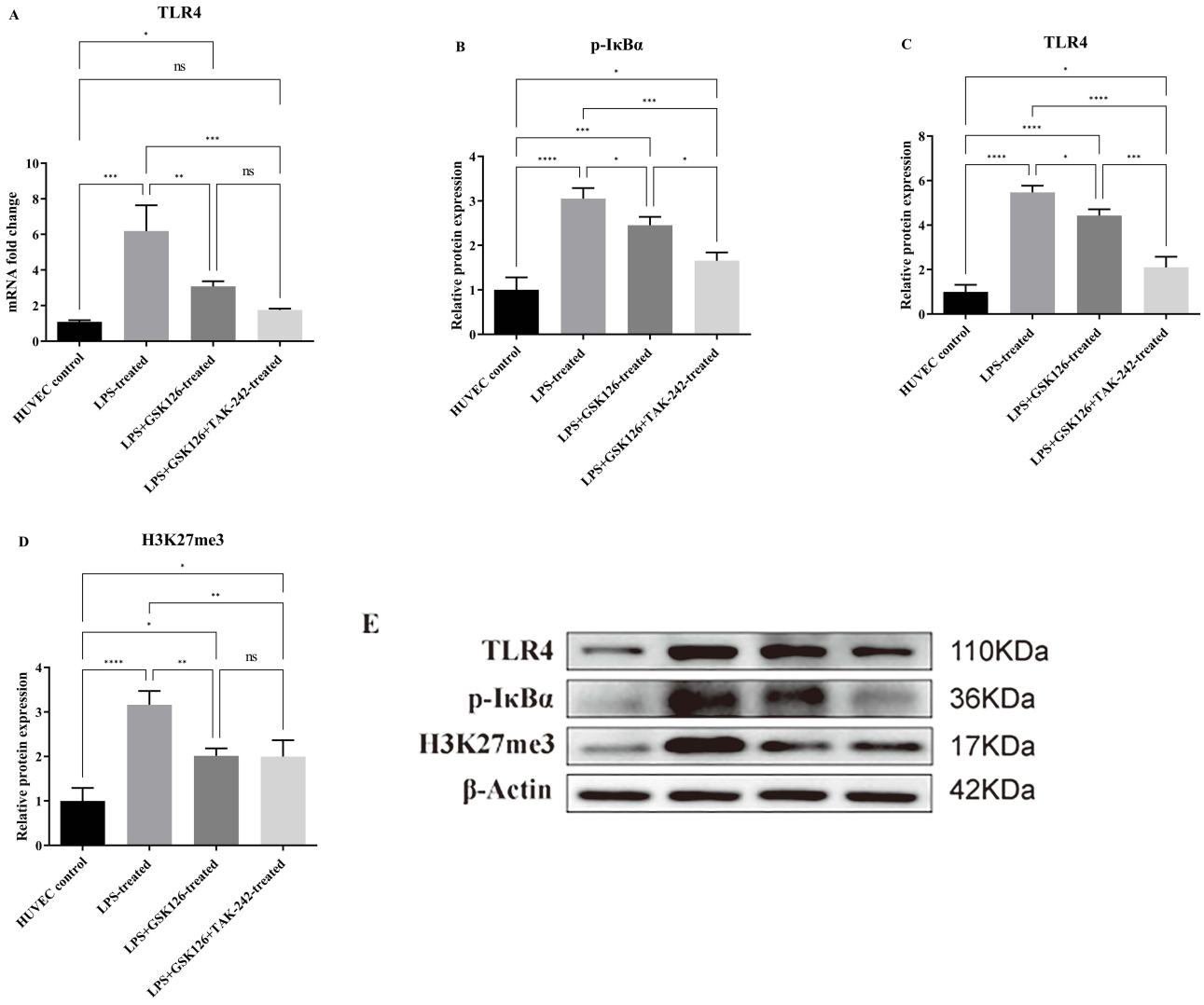

Figure 5 GSK126 inhibits LPS-induced TLR4 transcription and downstream signaling in HUVECs. (**A**) *TLR4* mRNA levels assessed by qPCR. LPS stimulation significantly increased *TLR4* mRNA expression (***p<0.001 vs control). GSK126 treatment significantly reduced the LPS-induced upregulation (**p<0.01 vs LPS). Importantly, co-treatment with TAK-242 further decreased *TLR4* mRNA expression to a level statistically indistinguishable from that of the control (p>0.05 vs control). (**B**–**D**) Quantification of protein levels. LPS stimulation robustly elevated TLR4 (**C**), phosphorylated IκBα (p-IκBα) (**B**), and H3K27me3 (**D**) protein levels (****p < 0.0001 vs control). GSK126 treatment significantly diminished both TLR4 and p-IκBα protein levels (*p < 0.05 vs LPS). The addition of TAK-242 produced an additional reduction in p-IκBα (*p < 0.05 vs GSK126 alone) and an even greater decrease in TLR4 (***p < 0.001 vs GSK126 alone). Consistent with effective EZH2 inhibition, GSK126 also significantly lowered H3K27me3 marks (**p<0.01 vs LPS). (**E**) Representative Western blots for TLR4, p-IκBα, and H3K27me3. β-actin served as the loading control.
Note: *p<0.05; **p<0.01; ***p<0.001; ***p<0.0001; ns, not significant.

diminished both proteins (p < 0.05 vs LPS), and the addition of TAK-242 produced an additional reduction in p-IκBα (p < 0.05) and an even greater decrease in TLR4 (p < 0.001 vs GSK126).

As expected, GSK126 also lowered global H3K27me3 marks in LPS-treated cells (p < 0.01, Figure 5D), confirming effective EZH2 inhibition. These protein-level changes were further supported by representative immunoblots (Figure 5E), which show the expression patterns of TLR4, p-IκBα, and H3K27me3 across different treatment conditions.

Collectively, these data support a model in which GSK126 modulates TLR4 signaling partly via the epigenetic downregulation of TLR4 transcription, whereas TAK-242 acts at the receptor and downstream signaling level (Figure 6).

https://doi.org/10.2147/JIR.S551388

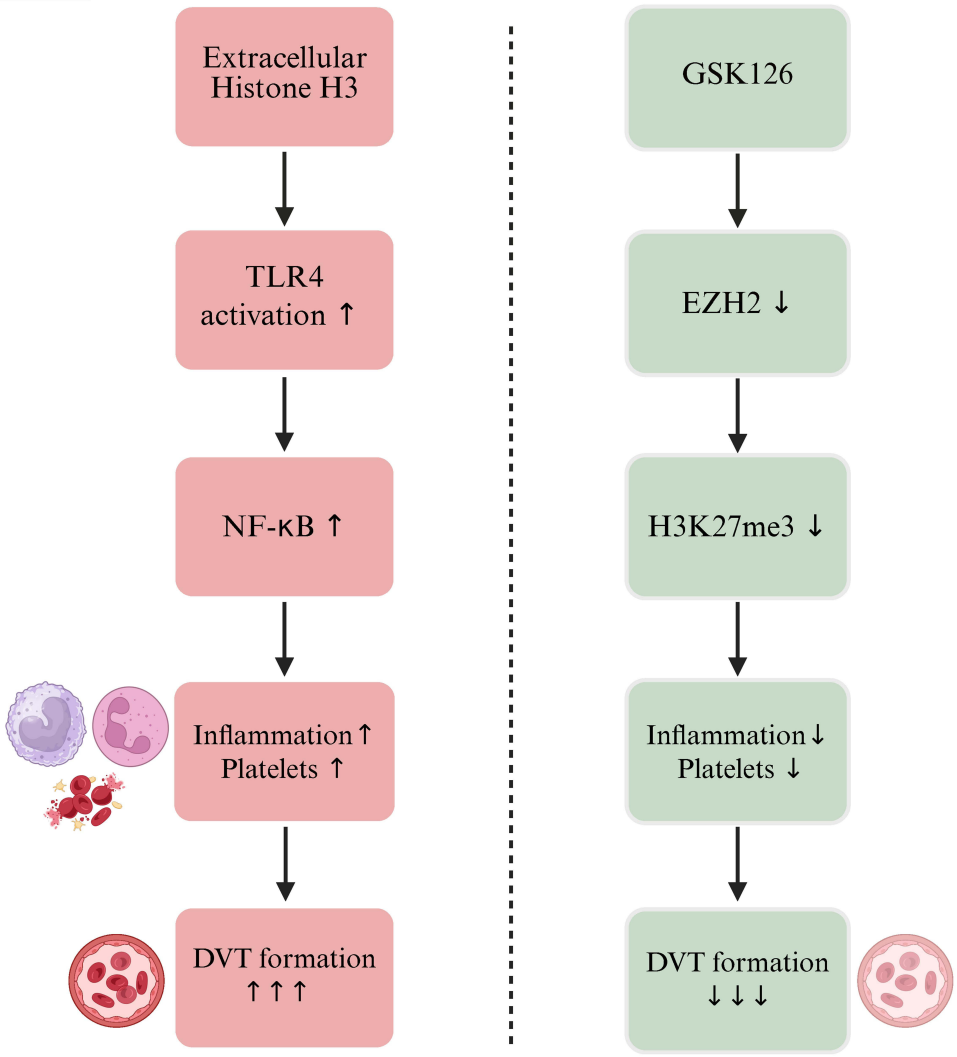

Figure 6 Proposed mechanism of GSK126-mediated inhibition of DVT formation.The pathological pathway (left) is initiated by extracellular histone H3, which activates the TLR4–NF-κB signaling cascade, and leads to inflammation, platelet activation, and ultimately the formation of deep vein thrombosis (DVT).The therapeutic pathway (right) illustrates how the EZH2 inhibitor GSK126 suppresses EZH2 activity, which results in reduced H3K27me3 levels and downstream attenuation of inflammation and platelet activation, thereby alleviating DVT formation.

Discussion

In this study, we found that GSK126, a specific EZH2 inhibitor, attenuated thromboinflammation in DVT by suppressing Tlr4-mediated endothelial and immune activation triggered by extracellular histone H3, thereby supporting the hypothesis that EZH2 may epigenetically regulate Tlr4 signaling during thrombosis. DVT develops within a complex microenvironment characterized by endothelial injury and immune activation. *Tlr4* plays a central role by sensing DAMPs, such as extracellular histone H3, and triggering downstream inflammatory cascades through MyD88 and TRIF pathways.[19] Consistent with earlier findings, we observed that histone H3 significantly increased the thrombus burden in wild-type mice. However, this effect was abolished in *Tlr4*-deficient animals, confirming the essential role of *Tlr4* in mediating H3-induced thrombosis.[12]

Our study also revealed that Tlr4 signaling contributed to endothelial activation in DVT. Markers such as E-selectin and vWF were significantly upregulated following H3 stimulation but were reduced in both the *Tlr4*-deficient and GSK126-treated groups. Among these markers, vWF exhibited a distinct expression pattern, with no significant difference between the $Tlr4^{-/-}$ + GSK126 and DVT + GSK126 groups. This contrasts with the clear reductions in IL-

6, VCAM-1, and E-selectin levels and suggests that vWF regulation may rely more specifically on Tlr4 signaling. These results collectively support the role of *Tlr4* in coordinating both endothelial dysfunction and systemic inflammation.[20,21]

GSK126, a specific EZH2 inhibitor, significantly reduced the expression of TLR4, proinflammatory cytokines (IL-6 and TNF-α), and adhesion molecules (VCAM-1 and ICAM-1) both in vivo and in vitro. These findings align with those of previous reports showing that EZH2 regulates proinflammatory gene expression through H3K27me3-mediated chromatin modifications.[22,23] Although we did not directly assess the H3K27me3 occupancy at the TLR4 locus, our observation of decreased H3K27me3 levels, together with suppressed TLR4 expression, supports a potential epigenetic mechanism. Further studies employing chromatin immunoprecipitation (ChIP) are warranted to confirm whether EZH2 directly modulates TLR4 promoter activity.

Interestingly, while previous studies suggested that EZH2 inhibition might affect extracellular histone levels,[24] GSK126 did not significantly reduce the plasma CitH3 level in our model. This may be due to the limited specificity of the ELISA used, which detects total CitH3 without resolving modification subtypes. Nevertheless, the observed reductions in the thrombus burden and inflammatory gene expression suggest that GSK126 functions downstream of histone release, most likely by modulating receptor-level responses or transcriptional activity.

Our experiments using TAK-242, performed exclusively in LPS-stimulated HUVECs, further confirmed that the anti-inflammatory effects of GSK126 were at least partially mediated through TLR4. Cotreatment with TAK-242 increased the suppression of TLR4 and downstream targets. However, differences between IL-6 and TNF-α responses were noted. IL-6 levels were further reduced by TAK-242, whereas TNF-α levels were not significantly affected, which suggested distinct regulatory pathways. Furthermore, TAK-242 fully restored ICAM-1 and P-selectin expression to baseline levels, indicating a strong TLR4 dependency of these adhesion molecules in endothelial cells.

Although LPS is a non-specific inflammatory stimulus, it is frequently used to simulate thromboinflammatory conditions in both in vitro and in vivo models. LPS induces endothelial cell activation through the TLR4–NF-κB signaling axis, which promotes cytokine release (eg, IL-6, TNF-α), upregulation of adhesion molecules (VCAM-1, E-selectin), and interactions with leukocytes and platelets.[25,26] These cellular responses are integral to the development of deep vein thrombosis and other thrombotic conditions. Therefore, LPS is a reproducible and mechanistically relevant tool for investigating upstream regulatory mechanisms such as EZH2-mediated modulation of TLR4 signaling.

Although our study focused on TLR4 as a primary mediator, the broader involvement of EZH2 in thromboinflammatory signaling is also of interest. Previous studies have shown that EZH2 can promote the transcription of IL-6, TNF-α, and oxidative stress-related genes through H3K27me3 enrichment under inflammatory conditions.[24,27] In hyperglycemic or autoimmune models, EZH2 activity exacerbates inflammation by reshaping chromatin accessibility. Our results, showing that GSK126 reduced both H3K27me3 levels and TLR4 expression, raise the possibility that epigenetic regulation may influence TLR4-mediated thromboinflammatory signaling in endothelial cells during thrombosis.

The specificity of GSK126 effects is further underscored by the divergent regulation of different inflammatory markers. For instance, the lack of additional TNF-α suppression by TAK-242 suggests the existence of a TLR4-independent component in TNF-α regulation, which potentially involves other PRRs or chromatin regulators. Moreover, the strong correlation between TLR4 and adhesion molecule expression suggests a more direct TLR4-mediated pathway for endothelial activation. These mechanistic nuances merit further investigation, particularly by using lineage-specific knockout models or transcriptomic profiling of endothelial and immune compartments, as TLR4 signaling may activate distinct downstream pathways in different cell types.[28]

From a translational perspective, the observed suppression of Tlr4 signaling and downstream cytokine expression makes GSK126 a promising candidate for modulating vascular inflammation. Tlr4 activation contributes to pathological inflammation not only in DVT but also in conditions such as acute liver injury, viral hepatitis, and COVID-19.[29,30] Although our findings are limited to a murine model of DVT, they may have broader implications for understanding how histone-induced Tlr4 signaling drives inflammation in diverse thromboinflammatory contexts.

Nonetheless, several limitations should be acknowledged. This study did not include a direct comparison between GSK126 and established anticoagulants for DVT, such as heparin, low-molecular-weight heparin, or direct oral anticoagulants (eg, rivaroxaban, apixaban). We also did not assess coagulation-related parameters (eg, PT, aPTT) or bleeding

risk, which are essential for evaluating anticoagulant efficacy and safety. As such, we cannot draw conclusions regarding the relative clinical utility of GSK126.

Importantly, unlike conventional anticoagulants that target the coagulation cascade, GSK126 modulates thromboinflammatory signaling and endothelial activation through EZH2 inhibition. This mechanistic distinction suggests that GSK126 may serve as a complementary rather than substitutive strategy, especially in settings where bleeding risk limits the use of traditional anticoagulants.

Additionally,we did not perform chromatin immunoprecipitation (ChIP) or promoter reporter assays, which limits the mechanistic precision of our conclusions. We also did not assess immune cell infiltration into thrombus or surrounding venous tissue, and therefore cannot determine whether GSK126 affects leukocyte recruitment in DVT. Future studies incorporating histological or flow cytometric analyses will be important to address this question. Although the observed reduction in H3K27me3 levels was accompanied by suppressed TLR4 expression, this correlation does not establish direct epigenetic regulation, and further chromatin-binding studies will be needed to confirm causality.

In addition, although GSK126 did not alter plasma CitH3 levels, the role of citrullinated histone H3 in Tlr4 activation remains unclear, especially given that the ELISA used cannot distinguish between modification subtypes. The long-term safety and therapeutic window of GSK126 in non-oncologic settings also remain to be established.

Due to the limited availability of $Tlr4^{-/-}$mice, in vivo experiments involving this genotype were conducted as a single cohort without biological replicates across batches. While internal consistency and statistical rigor were maintained, future validation in larger, independently repeated studies will be important. Furthermore, we did not assess the tissue localization or spatial co-localization of CitH3 and TLR4 in thrombus sections, which may provide valuable insight into their in situ interaction. Finally, because a $Tlr4^{-/-}$ + DVT group (without H3 stimulation) was not included in our design, we are unable to determine whether TLR4 deficiency alone alters baseline thrombus formation. This will be addressed in future investigations.

In conclusion, this study demonstrates that the EZH2 inhibitor GSK126 effectively alleviates thromboinflammation in deep vein thrombosis, a process associated with reduced H3K27me3 levels and suppression of TLR4-mediated inflammatory signaling. These results raise the possibility that epigenetic modulation may influence innate immune receptor expression in thrombosis. Further studies such as ChIP-seq or single-cell analysis are warranted to clarify whether EZH2 directly targets Tlr4 and to define cell-type-specific regulatory effects.

Human-Derived Cell Line

Human umbilical vein endothelial cells (HUVECs, BNCC342438) were purchased from BeNa Culture Collection. The cells were commercially obtained, de-identified, and do not contain any donor-identifiable information; therefore, their use was deemed exempt from ethical review by the Ethics Committee of Kunming Medical University.

Data Sharing Statement

The datasets and Supplementary Materials generated and/or analyzed during the current study are available from the corresponding author upon reasonable request.

Animal Ethics Approval

All animal experiments were approved by the Institutional Animal Care and Use Committee (IACUC) of Kunming Medical University and were conducted in accordance with the Regulations for the Administration of Affairs Concerning Experimental Animals (State Council of China, revised 2017) and the Laboratory Animal Welfare Ethical Review Guidelines (GB/T 35892–2018).

Author Contributions

All authors made a significant contribution to the work reported, whether that is in the conception, study design, execution, acquisition of data, analysis and interpretation, or in all these areas; took part in drafting, revising or critically reviewing the article; gave final approval of the version to be published; have agreed on the journal to which the article has been submitted; and agree to be accountable for all aspects of the work.

Funding

This work was supported by the General Project of Yunnan Basic Research Program (202301AT070104), the Joint Project of Kunming Medical University and Science and Technology Department of Yunnan Province (202101AY070001-119) and the Yunnan Clinical Center for Emergency Traumatic Diseases (YWLCYXZX2023300075). The funding body had no role in the study design, data collection, analysis, interpretation of data, or writing of the manuscript.

Disclosure

The authors declare that there are no conflicts of interest with any financial organization, corporation or individual that can inappropriately influence this work.

References

1. Merli GJ. Venous thromboembolism: commentary on prevention and treatment. *J Cardiovasc Nurs*. 2009;24(6):S1–3. doi:10.1097/JCN.0b013e3181b85ca6
2. Lurie JM, Png CYM, Subramaniam S, et al. Virchow's triad in "silent" deep vein thrombosis. *J Vasc Surg Venous Lymphat Disord*. 2019;7(5):640–645. doi:10.1016/j.jvsv.2019.02.011
3. Esmon CT. Basic mechanisms and pathogenesis of venous thrombosis. *Blood Rev*. 2009;23(5):225–229. doi:10.1016/j.blre.2009.07.002
4. Tritschler T, Kraaijpoel N, Le Gal G, et al. Venous thromboembolism: advances in diagnosis and treatment. *JAMA*. 2018;320(15):1583. doi:10.1001/jama.2018.14346
5. Varrias D, Palaiodimos L, Balasubramanian P, et al. The use of point-of-care ultrasound (POCUS) in the diagnosis of deep vein thrombosis. *J Clin Med*. 2021;10(17):3903. doi:10.3390/jcm10173903
6. Probeck K, Elitharp D, Condon C, et al. True failures of direct oral anticoagulants at a university medical center. *J Vasc Surg Venous Lymphat Disord*. 2022;10(2):561–562. doi:10.1016/j.jvsv.2021.12.044
7. Palareti G, Poli D. The challenges and limitations of widespread direct oral anticoagulant treatment: practical suggestions for their best use. *Expert Rev Cardiovasc Ther*. 2016;14(2):163–176. doi:10.1586/14779072.2016.1115344
8. Xu J, Zhang X, Monestier M, et al. Extracellular histones are mediators of death through TLR2 and TLR4 in mouse fatal liver injury. *J Immunol*. 2011;187(5):2626–2631. doi:10.4049/jimmunol.1003930
9. Mauracher L-M, Posch F, Martinod K, et al. Citrullinated histone H3, a biomarker of neutrophil extracellular trap formation, predicts the risk of venous thromboembolism in cancer patients. *J Thromb Haemost*. 2018;16(3):508–518. doi:10.1111/jth.13951
10. Zhu YP, Speir M, Tan Z, et al. NET formation is a default epigenetic program controlled by PAD4 in apoptotic neutrophils. *Sci Adv*. 2023;9(51):eadj1397. doi:10.1126/sciadv.adj1397
11. Liu L, Zhang W, Su Y, et al. The impact of neutrophil extracellular traps on deep venous thrombosis in patients with traumatic fractures. *Clin Chim Acta*. 2021;519:231–238. doi:10.1016/j.cca.2021.04.021
12. Kim J, Baalachandran R, Li Y, et al. Circulating extracellular histones exacerbate acute lung injury by augmenting pulmonary endothelial dysfunction via TLR4-dependent mechanism. *Am J Physiol Lung Cell Mol Physiol*. 2022;323(3):L223–39. doi:10.1152/ajplung.00072.2022
13. Semeraro F, Ammollo CT, Morrissey JH, et al. Extracellular histones promote thrombin generation through platelet-dependent mechanisms: involvement of platelet TLR2 and TLR4. *Blood*. 2011;118(7):1952–1961. doi:10.1182/blood-2011-03-343061
14. Yuan H, Huang X, Ding J, et al. Toll-like receptor 4 deficiency in mice impairs venous thrombus resolution. *Front Mol Biosci*. 2023;10:1165589. doi:10.3389/fmolb.2023.1165589
15. Wang Z, Wang F, Kong X, et al. Oscillatory shear stress induces oxidative stress via TLR4 activation in endothelial cells. *Mediators Inflamm*. 2019;2019:7162976. doi:10.1155/2019/7162976
16. Bonfiglio CA, Lacy M, Janjic A, et al. The role of EZH2 and H3K27me3 epigenetic signature in modulating T-cell polarization in atherosclerosis. *Eur Heart J*. 2023;44(Suppl 2):ehad655.3232. doi:10.1093/eurheartj/ehad655.3232
17. Liu Y, Zhang Q, Ding Y, et al. Histone lysine methyltransferase Ezh1 promotes TLR-triggered inflammatory cytokine production by suppressing Tollip. *J Immunol*. 2015;194(6):2838–2846. doi:10.4049/jimmunol.1402087
18. Huang S, Wang Z, Zhou J, et al. EZH2 inhibitor GSK126 suppresses antitumor immunity by driving production of myeloid-derived suppressor cells. *Cancer Res*. 2019;79(8):2009–2020. doi:10.1158/0008-5472.CAN-18-2395
19. Stierschneider A, Wiesner C. Shedding light on the molecular and regulatory mechanisms of TLR4 signaling in endothelial cells under physiological and inflamed conditions. *Front Immunol*. 2023;14:1264889. doi:10.3389/fimmu.2023.1264889
20. Ramasubramanian B, Kim J, Ke Y, et al. Mechanisms of pulmonary endothelial permeability and inflammation caused by extracellular histone subunits H3 and H4. *FASEB J*. 2022;36(9):e22470. doi:10.1096/fj.202200303RR
21. Pérez-Cremades D, Bueno-Betí C, García-Giménez JL, et al. Extracellular histones trigger oxidative stress-dependent induction of the NF-kB/CAM pathway via TLR4 in endothelial cells. *J Physiol Biochem*. 2023;79(2):251–260. doi:10.1007/s13105-022-00935-z
22. Kempkes RWM, Rief LCM, Roomen CPAA, et al. EZH2 inhibition reduces macrophage inflammatory responses in atherosclerosis. *Atherosclerosis*. 2023;364:e10. doi:10.1016/j.atherosclerosis.2023.06.085
23. Kunanopparat A, Leelahavanichkul A, Visitchanakun P, et al. The regulatory roles of Ezh2 in response to lipopolysaccharide (LPS) in macrophages and mice with conditional Ezh2 deletion with LysM-Cre system. *Int J Mol Sci*. 2023;24(6):5363. doi:10.3390/ijms24065363
24. Sánchez-Ceinos J, Hussain S, Khan AW, et al. Repressive H3K27me3 drives hyperglycemia-induced oxidative and inflammatory transcriptional programs in human endothelium. *Cardiovasc Diabetol*. 2024;23(1):122. doi:10.1186/s12933-024-02196-0
25. Zhang X, Li Y, Yang X, et al. Circulating LPS from gut microbiota leverages stenosis-induced deep vein thrombosis in mice. *Cell Commun Signal*. 2023. 21(1):59. doi: 10.1186/s12964-023-01070-6.

26. Li L, Li M, Yang J, et al. Bacterial lipopolysaccharide-induced endothelial activation and dysfunction: a new predictive and therapeutic paradigm for sepsis. *Signal Transduct Target Ther*. 2023;8(1):313. doi: 10.1038/s41392-023-01527-z.
27. Qu D, Wang L, Huo M, et al. Focal TLR4 activation mediates disturbed flow-induced endothelial inflammation. *Cardiovasc Res*. 2020;116 (1):226–236. doi:10.1093/cvr/cvz046
28. Ishida I, Kubo H, Suzuki S, et al. Hypoxia diminishes toll-like receptor 4 expression through reactive oxygen species generated by mitochondria in endothelial cells. *J Immunol*. 2002;169(4):2069–2075. doi:10.4049/jimmunol.169.4.2069
29. Tang YL, Zhu L, Tao Y, et al. Role of targeting TLR4 signaling axis in liver-related diseases. *Pathol Res Pract*. 2023;244:154410. doi:10.1016/j.prp.2023.154410
30. Aboudounya MM, Heads RJ. COVID-19 and toll-like receptor 4 (TLR4): SARS-CoV-2 may bind and activate TLR4 to increase ACE2 expression, facilitating entry and causing hyperinflammation. *Mediators Inflamm*. 2021;(2021):8874339. doi:10.1155/2021/8874339